Sphingosine kinase 1 overexpression induces MFN2 fragmentation and alters mitochondrial matrix Ca2+ handling in HeLa cells

Pulli, Ilari

2019-09

Pulli , I , Lof , C , Blom , T , Asghar , M Y , Lassila , T , Back , N , Lin , K-L , Nystrom , J H , Kemppainen , K , Toivola , D M , Dufour , E , Sanz , A , Cooper , H M , Parys , J B & Tornquist , K 2019 , ' Sphingosine kinase 1 overexpression induces MFN2 fragmentation and alters mitochondrial matrix Ca2+ handling in HeLa cells ' , Biochimica et Biophysica Acta. Molecular Cell Research , vol. 1866 , no. 9 , pp. 1475-1486 . https://doi.org/10.1016/j.bbamcr.2019.06.006

http://hdl.handle.net/10138/318773
https://doi.org/10.1016/j.bbamcr.2019.06.006

unspecified
publishedVersion

BBA - Molecular Cell Research 1866 (2019) 1475–1486

Contents lists available at ScienceDirect

BBA - Molecular Cell Research

journal homepage: www.elsevier.com/locate/bbamcr

Sphingosine kinase 1 overexpression induces MFN2 fragmentation and alters mitochondrial matrix Ca^{2+} handling in HeLa cells

I. Pulli[a], C. Löf[b], T. Blom[c,g], M.Y. Asghar[a,g], T. Lassila[a,g], N. Bäck[c], K.-L. Lin[a], J.H. Nyström[a], K. Kemppainen[a], D.M. Toivola[a], E. Dufour[d], A. Sanz[e], H.M. Cooper[a], J.B. Parys[f], K. Törnquist[a,g,*]

[a] Åbo Akademi University, Faculty of Science and Engineering, Biosciences, Tykistökatu 6A, 20520 Turku, Finland
[b] University Of Turku, Research Centre for Cancer, Infections and Immunity, Institute of Biomedicine, Kiinamyllynkatu 10, 20520 Turku, Finland
[c] Department of Anatomy, Faculty of Medicine, University of Helsinki, 00014 Helsinki, Finland
[d] University of Tampere 33520, Tampere, Finland
[e] Newcastle University Institute for Ageing, Newcastle upon Tyne NE4 5PL, United Kingdom of Great Britain and Northern Ireland
[f] Laboratory of Molecular and Cellular Signaling, Department of Cellular and Molecular Medicine, KU Leuven, Leuven, Belgium
[g] Minerva Foundation Institute For Medical Research, Biomedicum Helsinki, 00270 Helsinki, Finland

ARTICLE INFO

Keywords:
Mitochondria
Calcium
Sphingosine kinase 1
Sphingosine 1-phosphate
Mitofusin-2
Endoplasmic reticulum

ABSTRACT

Sphingosine kinase 1 (SK1) converts sphingosine to the bioactive lipid sphingosine 1-phosphate (S1P). S1P binds to G-protein-coupled receptors ($S1PR_{1-5}$) to regulate cellular events, including Ca^{2+} signaling. The SK1/S1P axis and Ca^{2+} signaling both play important roles in health and disease. In this respect, Ca^{2+} microdomains at the mitochondria-associated endoplasmic reticulum (ER) membranes (MAMs) are of importance in oncogenesis. Mitofusin 2 (MFN2) modulates ER-mitochondria contacts, and dysregulation of MFN2 is associated with malignancies. We show that overexpression of SK1 augments agonist-induced Ca^{2+} release from the ER resulting in increased mitochondrial matrix Ca^{2+}. Also, overexpression of SK1 induces MFN2 fragmentation, likely through increased calpain activity. Further, expressing putative calpain-cleaved MFN2 N- and C-terminal fragments increases mitochondrial matrix Ca^{2+} during agonist stimulation, mimicking the SK1 overexpression in cells. Moreover, SK1 overexpression enhances cellular respiration and cell migration. Thus, SK1 regulates MFN2 fragmentation resulting in increased mitochondrial Ca^{2+} and downstream cellular effects.

1. Introduction

Sphingosine kinase 1 (SK1) is a lipid kinase involved in multiple pathologies, including cancer and severe neurological conditions [1,2]. SK1 acts by converting sphingosine into the signaling lipid sphingosine 1-phosphate (S1P), which is exported to the extracellular space for auto/paracrine stimulation of the G-protein coupled S1P receptors 1–5 ($S1PR_{1-5}$). S1P has been shown to have direct intracellular effects, including modulation of intracellular calcium (Ca^{2+}) signaling. Also, there is evidence for the inter-regulation of SK1/S1P and Ca^{2+} signaling, as SK1 activation is in part modulated by Ca^{2+} [3,4]. Being a ubiquitous second messenger, Ca^{2+} regulates a wide variety of cellular functions, such as proliferation, migration, respiration, neuronal function and cell death [5–8]. Aberrant intracellular Ca^{2+} signaling may thus lead to pathological effects. The regulation of Ca^{2+} signaling is tightly controlled and compartmentalized. The main intracellular Ca^{2+} store is the endoplasmic reticulum (ER). Also, mitochondria are important players in intracellular Ca^{2+} handling, as they readily take up Ca^{2+} and can act as Ca^{2+} buffers or sinks [9,10]. Importantly, Ca^{2+} is a key regulator of mitochondrial enzymes involved in ATP production [7]. On the other hand, mitochondrial Ca^{2+} overload may lead to programmed cell death [11]. Interactions between the ER and the mitochondria are regulated at specific membrane contact sites between the two organelles. The sites of the ER-membranes that are involved in this inter-organellar regulation are thus named mitochondria-associated membranes, or MAMs. For instance, lipid transfer and Ca^{2+} flux are coordinated at the MAM sites [12,13]. Several proteins, including mitofusin 2 (MFN2), have been found to reside at and to regulate the dynamics of the MAM contacts [13,14]. Interestingly, opposing findings concerning the effect of MFN2 expression/depletion on ER-mitochondria tethering and mitochondrial Ca^{2+} signaling have been reported [14–20].

The concept and importance of compartmentalized intracellular Ca^{2+} signaling is actively studied with much emphasis put on the ER-

* Corresponding author.
E-mail address: Kid.Tornqvist@abo.fi (K. Törnquist).

https://doi.org/10.1016/j.bbamcr.2019.06.006
Received 15 October 2018; Received in revised form 2 June 2019; Accepted 13 June 2019
Available online 17 June 2019

mitochondria interactions and mitochondrial Ca^{2+} uptake [21,22]. Interestingly, S1P signaling is linked to mitochondrial biology. It has been reported that S1P produced by the sphingosine kinase 2 (SK2) isoform modulates mitochondrial respiration and antagonizes the opening of the mitochondrial permeability transition pore (mPTP) in ischemic heart tissue [23,24]. Also, S1P treatment (0.5–2 mg/kg) after experimental heart ischemia/reperfusion in rats suppresses the mPTP opening and thus maintains the mitochondrial membrane potential, which blunts the ischemic reperfusion injury [25]. Further, SK1 has been recently shown to localize to mitochondria to activate the mitochondrial unfolded protein response in *C. elegans* [26]. Also, inhibition of SK1 through reduced S1P levels induces mitochondrial dysfunction in pancreatic β-cells [27]. As mentioned earlier, S1P has been shown to affect Ca^{2+} handling through unknown intracellular mechanisms as well as through the G-protein coupled S1P-receptors. Upon activation, the $S1PR_{1-4}$ couple to phospholipase C (PLC) to induce inositol trisphosphate (IP_3) generation which is followed by Ca^{2+} release from the ER through the IP_3-receptors [3]. Mitochondrial uptake of Ca^{2+} that is released from the ER is coordinated at the MAM contact sites [28]. Further, altered SK1/S1P signaling as well as disrupted Ca^{2+} signaling in the mitochondrial matrix and at the MAM sites, respectively, have strong oncogenic implications [1,11,22,29]. Taken together, these observations led us to test whether SK1 overexpression would affect Ca^{2+} handling at the ER-mitochondria compartments. For this, we used a previously established HeLa cell model [30] overexpressing human SK1 (hSK1), and genetically targeted aequorins for the Ca^{2+} measurements [31]. We previously showed that the $[Ca^{2+}]$ in caveolin-1 (Cav-1)-enriched microdomains was augmented by hSK1 overexpression as reported by the luminescent chimeric Cav-1-aequorin [30]. However, SK1 overexpression did not significantly increase the cytoplasmic $[Ca^{2+}]$ in HeLa cells during histamine-induced Ca^{2+} release [30]. Hence, in the present study, we characterized the effects of SK1 overexpression on ER lumen ($[Ca^{2+}]_{ER}$) and mitochondrial matrix Ca^{2+} concentrations ($[Ca^{2+}]_{mit}$).

2. Results

2.1. SK1 augments ER Ca^{2+} release and mitochondrial Ca^{2+} uptake

First, we examined mitochondrial matrix and luminal ER Ca^{2+} concentrations in mock-transduced and SK1-overexpressing (hSK1) HeLa cells. The HeLa cell lines were as described in [30], and the SK1 overexpression is shown in Supplementary Fig. 1. The cells were challenged with the IP_3-generating agonist histamine (100 μM) in the presence of the Ca^{2+} chelator EGTA (150 μM) in the extracellular buffer. EGTA was added directly prior to the agonist stimulation to avoid unwanted emptying of the intracellular Ca^{2+} stores, and importantly, to eliminate extracellular Ca^{2+} as a source for cytoplasmic Ca^{2+} entry during agonist stimulation. In this experimental setting, both the release of ER Ca^{2+} as well as the Ca^{2+} uptake to the mitochondrial matrix were significantly augmented in SK1-overexpressing cells (Fig. 1A, B). $[Ca^{2+}]_{mit}$ was significantly higher in hSK1 cells upon histamine stimulation also when 1 mM Ca^{2+} was present in the extracellular buffer solution (Fig. 1C). These results indicate that the increased ER-derived Ca^{2+} is effectively shunted to the mitochondria in SK1-overexpressing cells. This is further highlighted by the previous results from our group [30] that showed no SK1-induced changes in the cytoplasmic Ca^{2+}. Of note, SK1-overexpression did not lead to marked changes in the IP_3-receptor protein levels, indicating that the increased release of ER Ca^{2+} during histamine stimulation was not due to altered IP_3R expression (Suppl. Fig. 1). Importantly, also transient SK1-overexpression in both HeLa and FTC-133 cell lines led to increased mitochondrial Ca^{2+} uptake upon agonist stimulation (Suppl. Fig. 2A, B; and see Suppl. Fig. 5).

We then examined the possibility that SK1 overexpression would affect the mitochondrial Ca^{2+} uptake *per se*. For this, the cells were permeabilized by digitonin treatment in the presence of an intracellular buffer (IB, supplemented with ATP) containing EGTA to chelate Ca^{2+} [31]. After plasma membrane permeabilization, the cells were perfused with IB containing 4 μM free Ca^{2+} to allow for mitochondrial Ca^{2+} uptake [31]. In this setting, SK1 overexpression had no effect on $[Ca^{2+}]_{mit}$ as compared to the mock-transduced cells (Fig. 2A). This finding is in line with the observation that SK1 overexpression did not markedly alter the expression levels of the proteins involved in mitochondrial matrix Ca^{2+} handling that were tested (MCU [32], MICU1 [33], MCUR1 [34], NCLX [35], AFG3L2 [36], OPA1 [37], Suppl. Fig. 1). Next, we treated mock-transduced and SK1-overexpressing cells with the ionophore ionomycin in the presence of EGTA. In this experiment, the intracellular Ca^{2+} released by the ionomycin treatment accumulated to a greater extent in the matrix of SK1-overexpressing cell mitochondria (Fig. 2B). The effect of SK1 overexpression was more pronounced when the cells were briefly incubated with the cytoplasmic Ca^{2+} chelator BAPTA-AM prior to the ionomycin treatment (Fig. 2C). Importantly, cytoplasmic calcium was unaffected in SK1-overexpressing cells upon ionomycin treatment in the presence of EGTA (Fig. 2D). These data thus suggest that SK1-overexpression augments the shunting of intracellularly stored Ca^{2+} to the mitochondria, whereas the intrinsic mitochondrial Ca^{2+} uptake capacity in permeabilized cells is not altered by SK1.

2.2. SK1 overexpression induces cleavage of mitofusin-2

As we did not see any changes in the mitochondrial inner membrane Ca^{2+} handling proteins, we asked whether SK1 affects the expression of mitofusin-2 (MFN2), an essential regulator of mitochondrial fusion and mitochondria-ER interactions at the MAM sites [38]. We found that the levels of full-length MFN2 (~80 kDa) were not altered, but observed that the SK1-overexpressing cells showed a distinct protein fragment recognized by the N-terminal targeting anti-MFN2 antibody (Fig. 3A). Intriguingly, calpain has been reported to induce MFN2 fragmentation [39] and calpain is activated by S1P and an S1P analogue [40,41]. In agreement with this, we observed an increase in calpain activity in SK1-overexpressing cells (Fig. 3B). Of note, calpain activity was increased, and a MFN2-fragment was identified, in HeLa and FTC-133 cells upon transient SK1 overexpression. Further, long-term SK1-inhibitor treatment reduced MFN2 fragment expression levels (Suppl. Fig. 3). MFN2 contains multiple putative calpain cleavage sites with the highest score predicted for cleavage between the His467 and Arg468 residues (prediction based on ref. [42] and conducted with the online tools at www.calpain.org). Hence, we generated plasmid constructs to express MFN2 fragments that would result from calpain-mediated cleavage at the putative His467-Arg468 site (Fig. 3C). Of note, the resulting fragments include intact active domains of the full-length protein: the N-terminal fragment harbors the GTPase, coiled-coil heptad repeat (HR1) and proline rich (PR) domains, whereas the transmembrane (TM) and HR2 domains reside in the C-terminal fragment (see Fig. 3C and ref. [14] for a schematic representation). Interestingly, the expression of both the N- and C-terminal MFN2 fragments, respectively, was found to augment the mitochondrial Ca^{2+} uptake (Fig. 3D), and similar results were obtained when the FTC-133 cell line was used (Suppl. Fig. 2C). In contrast, cytoplasmic Ca^{2+} was unaffected by MFN2 fragment expression (Fig. 3E). These results indicate that the MFN2 fragments are biologically active and are able to modulate mitochondrial physiology in a manner that is coupled to mitochondrial Ca^{2+} uptake. Importantly, this is in agreement with the previous reports that have shown MFN2 fragment/mutant expression or MFN2-derived cell permeable short peptides to be biologically active and to affect mitochondrial function [43–45].

2.3. Mitochondrial Na^+/Ca^{2+} exchanger activity is reduced by SK1 overexpression

The mitochondrial Na^+/Ca^{2+} exchanger protein (NCLX) regulates

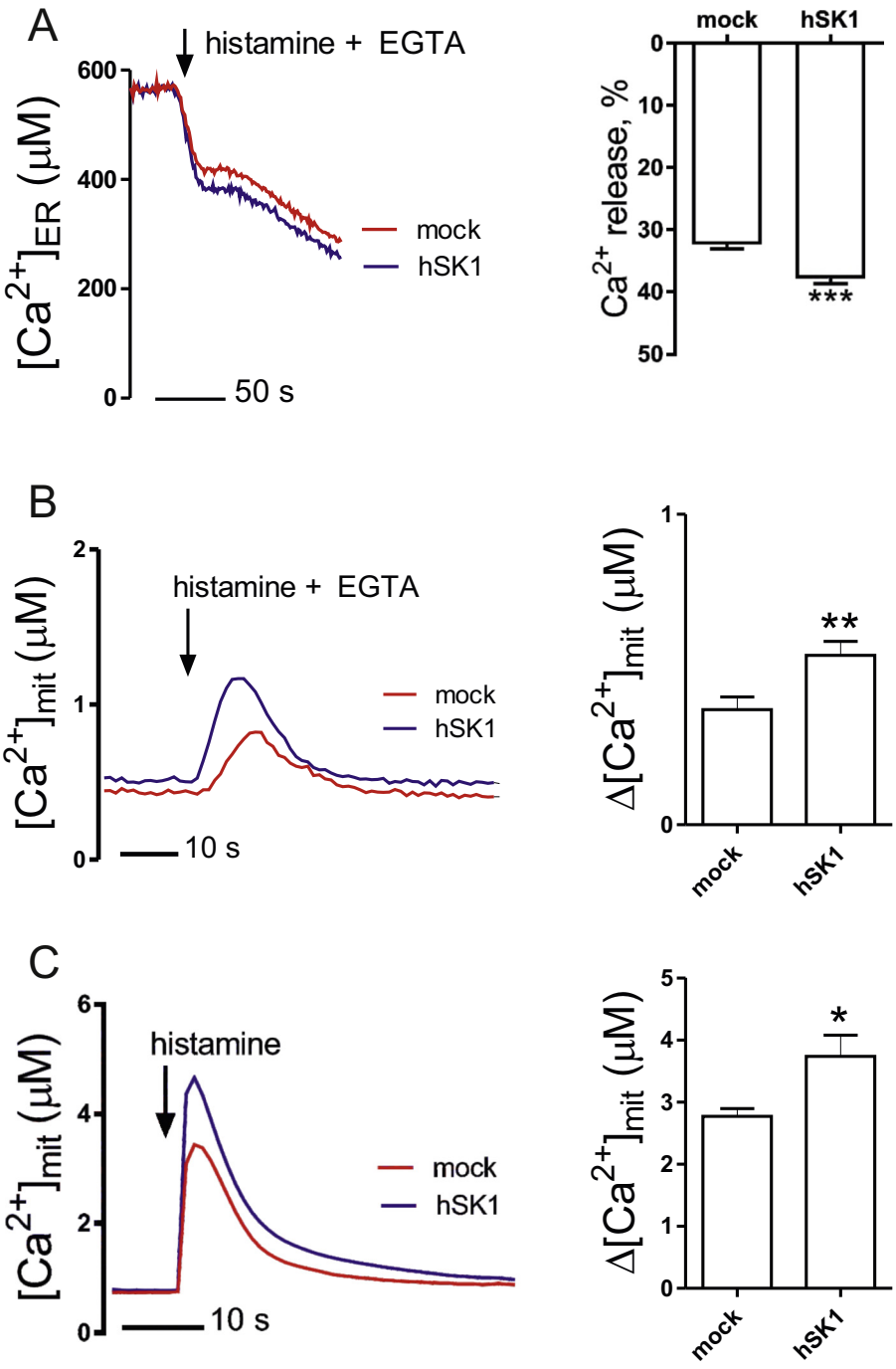

Fig. 1. The effect of SK1 overexpression on ER Ca^{2+} release and mitochondrial Ca^{2+} uptake. A) Histamine-induced Ca^{2+} release from the ER is greater in SK1-overexpressing HeLa cells than in the mock-transduced controls. Targeted aequorins as described in Section 4.2 were employed for Ca^{2+} measurements in these compartments. The baseline ER Ca^{2+} of the cells was recorded in an HBSS buffer containing 1 mM Ca^{2+}. Thereafter, the cells were perfused with HBSS containing 100 μM histamine and 150 μM EGTA when indicated by the arrow to induce a rapid IP_3-mediated Ca^{2+} release from the ER. Representative traces and quantification with S.E.M of the percental ER Ca^{2+} release are shown, N = 8 for mock, N = 9 for hSK1, ***P < 0.001. B) Mitochondrial Ca^{2+} was measured upon 100 μM histamine treatment in the presence of 150 μM EGTA in the buffer. Representative traces and quantification of the change (Δ, delta) in $[Ca^{2+}]_{mit}$ from basal to maximal stimulated concentration are shown, N = 11, **P < 0.01. C) Mitochondrial Ca^{2+} was measured after 100 μM histamine treatment in the presence of 1 mM Ca^{2+} in the buffer. Representative traces and quantification of $\Delta[Ca^{2+}]_{mit}$ are shown, N = 7, *P < 0.01.

the Ca^{2+} efflux from the mitochondrial matrix in a Na^+-dependent manner, and consequently, NCLX-inhibition leads to accumulation of Ca^{2+} in the matrix [35,46]. Interestingly, the involvement of MFN2 in the regulation of mitochondrial matrix Ca^{2+} by modulating the activity of NCLX has been reported [47]. We conducted mitochondrial Ca^{2+} recordings during increasing agonist concentrations to study the kinetics of $[Ca^{2+}]_{mit}$ upon repeated increases in intracellular $[Ca^{2+}]$. In this experiment, SK1-overexpressing cells again showed increased $[Ca^{2+}]_{mit}$ compared to the mock-transduced cells (Fig. 4A). To assess the possible involvement of NCLX, the cells were treated with the NCLX inhibitor CGP-37157 (CGP). Blocking NCLX did not significantly affect the $[Ca^{2+}]_{mit}$ in cells overexpressing SK1, whereas the mock-transduced cells showed an increase in $[Ca^{2+}]_{mit}$ when NCLX was inhibited (Fig. 4B). This experiment suggests that the basal NCLX activity is low in SK1-overexpressing cells, contributing, at least in part, to the accumulation of Ca^{2+} in the mitochondrial matrix.

2.4. Overexpression of SK1 or the MFN2 N- and C-terminal fragments has no effect on mitochondrial-ER networks

As mitochondria-ER dynamics regulates Ca^{2+} signaling, we set out to investigate whether SK1 or MFN2 N- and C-terminal fragment overexpression, respectively, would have an effect on these organelles. First, SK1 overexpression showed no significant effects on the appearance of the ER-mitochondria networks as visualized by immunofluorescence and confocal microscopy (Fig. 5A). The expression of MFN2 N- and C- terminal fragments did not have an effect on the mitochondrial network, whereas full-length MFN2 expression resulted in

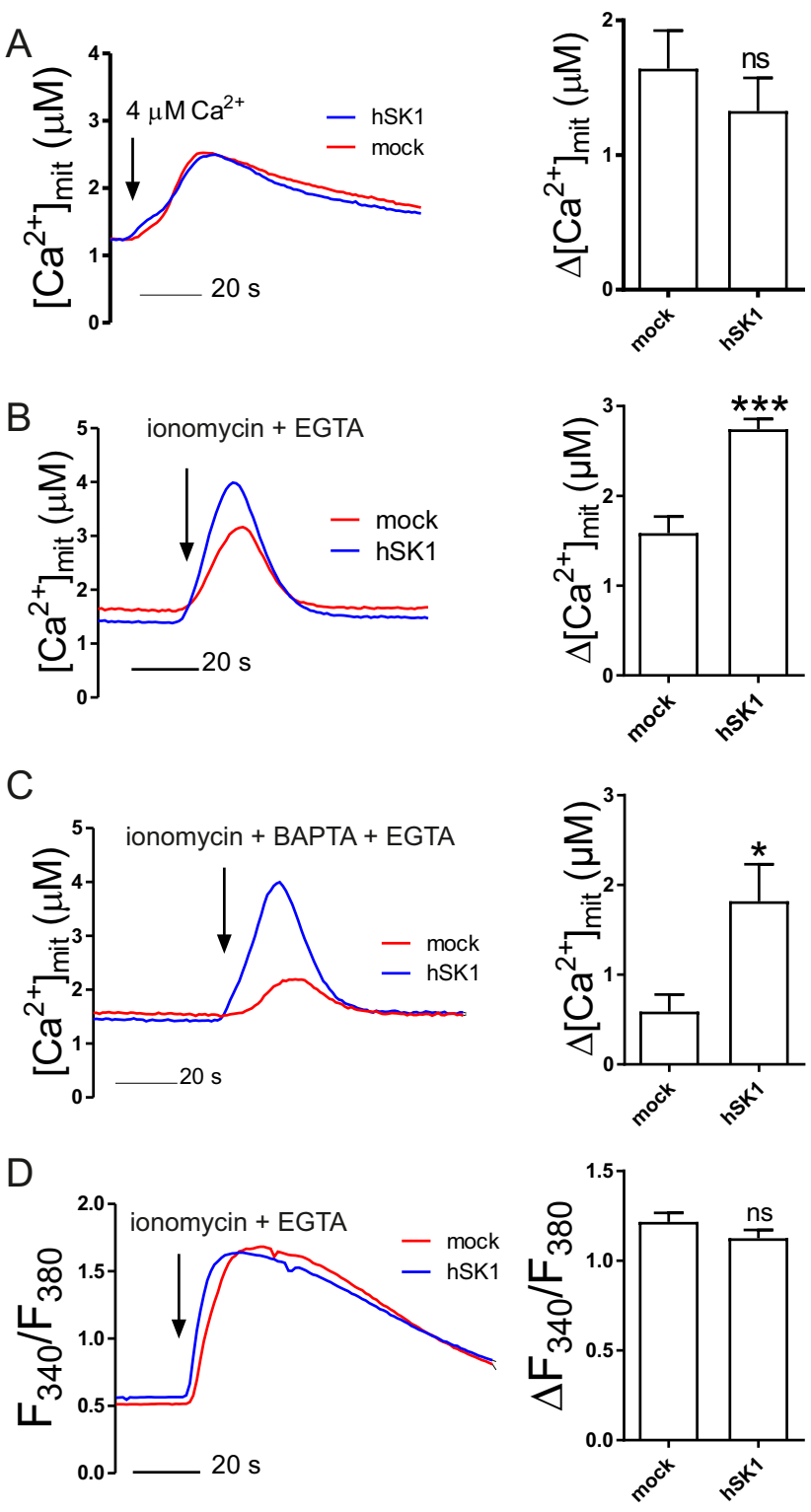

Fig. 2. Effect of SK1 overexpression on mitochondrial Ca^{2+} in permeabilized cells during Ca^{2+} addition as well as in intact cells during ionomycin treatment. Mitochondria-targeted aequorin was employed in the experiment shown in panels A–C, whereas the Ca^{2+} indicator Fura-2-AM was used for the measurements shown in panel D, see Section 4.2. A) To permeabilize the plasma membrane, the cells were treated with 25 μM digitonin in an intracellular buffer (IB, see the text and ref. [31]) in the presence of EGTA. Then, the cells were perfused with IB containing 4 μM free Ca^{2+} to allow for mitochondrial Ca^{2+} uptake (as described in [31]. In this setting, no significant differences between hSK1 and mock-transduced cells could be detected, N = 9 for mock, N = 8 for hSK1. B) The cells were treated with 5 μM ionomycin in the presence of 150 μM EGTA in the extracellular buffer when indicated by the arrow. $[Ca^{2+}]_{mit}$ was significantly higher in SK1-overexpressing cells, N = 4 for mock, N = 5 for hSK1. C) The cells were pretreated with BAPTA-AM for 2.5 min prior to treating the cells with 5 μM ionomycin in the presence of 150 μM EGTA. The brief BAPTA-AM treatment resulted in significant reduction in ionomycin-induced $[Ca^{2+}]_{mit}$ in the mock-transduced cells as compared to the SK1-overexpressing cells, N = 5 for mock, N = 6 for hSK1. D) Cytoplasmic Ca^{2+} was not affected by SK1 overexpression during 5 μM ionomycin treatment in the presence of 150 μM EGTA in the extracellular buffer, N = 4. The bar diagrams show the average of the change (Δ) from basal to maximal $[Ca^{2+}]_{mit}$ recorded during each experiment. The error bar shows S.E.M. * = $P < 0.05$, *** = $P < 0.001$, ns = not significant.

the previously reported mitochondrial clustering [44,48] (Fig. 5B). Of note, SK1-GFP did not colocalize with the mitochondria (Fig. 5C). Further, we performed electron microscopy to analyze the mitochondria-ER network. In agreement with the results obtained by confocal microscopy, the mitochondrial surface area or the mitochondria-ER contacts were not affected by SK1 overexpression as evidenced by the electron microscopy approach (Fig. 6).

2.5. SK1 does not affect proliferation but increases cell respiration and migration

Finally, we set out to characterize other possible physiological effects of SK1 overexpression. As Ca^{2+} is an important regulator of metabolism and mitochondrial ATP production, we measured cellular respiration. We found that SK1 overexpression slightly but significantly increased the basal oxygen consumption in HeLa cells (Fig. 7A). Further, mitochondrial Ca^{2+} is of importance in the regulation of cancer

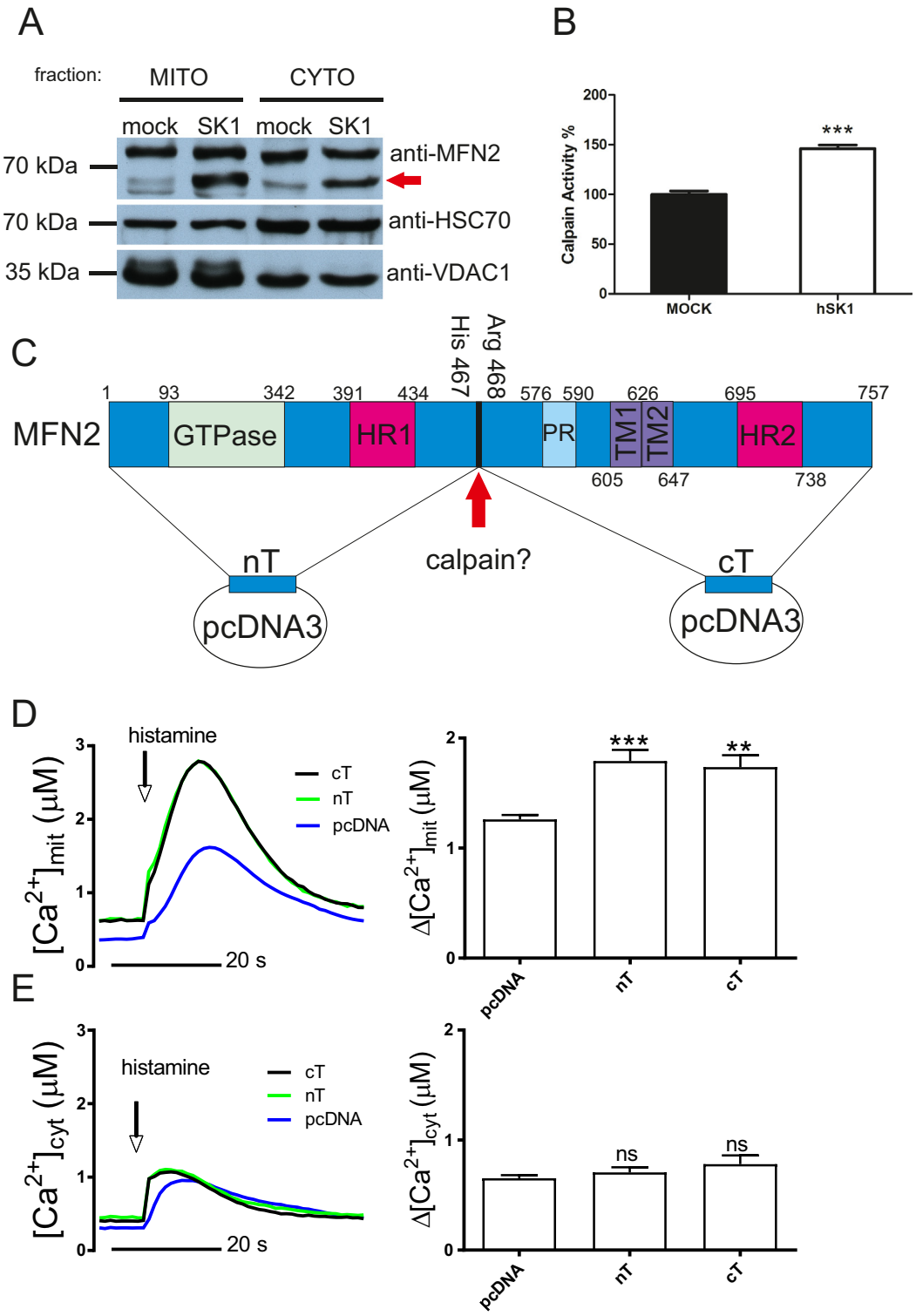

Fig. 3. Mitofusin-2 is fragmented in SK1-overexpressing cells, and transient MFN2 fragment expression increases mitochondrial Ca^{2+}. Mitochondria-targeted, or non-targeted (cytoplasmic) aequorin was employed in the Ca^{2+} experiments shown. A) Western blot analysis revealed the presence of a fragment of MFN2 protein in lysates of SK1-overexpressing cells. The fragmented MFN2, indicated by the red arrow, was present both in the mitochondrial fraction and in the whole cell lysate of cells overexpressing SK1. HSC70 and the mitochondrial outer membrane protein, VDAC1, served as loading controls. B) Calpain activity was increased in cells overexpressing SK1 (%, mock-cells normalized to 100%). N = 5, ***P < 0.001. C) Schematic presentation of MFN2 with the functional domains, adapted from [14]. The predicted calpain cleavage site is between Arginine 468 and Histidine 467 of MFN2. Plasmid expression vectors (pcDNA3) carrying the N- and C-terminal parts of MFN2 that would result after calpain cleavage at the indicated site (red arrow) were created. GTPase = GTPase domain; HR1, HR2 = heptad-repeat domains; PR = proline-rich domain; TM1, TM2 = transmembrane domains. D) Expression of the N- and C-terminal plasmid constructs augmented mitochondrial Ca^{2+} uptake, whereas cytoplasmic Ca^{2+} was unaffected in these conditions (E), N = 14 in D & E. The change in Ca^{2+} concentration from basal to maximal stimulated concentration is quantified in the bar diagrams. The error bars show the S.E.M. **P < 0.01, ***P < 0.001, ns = not significant.

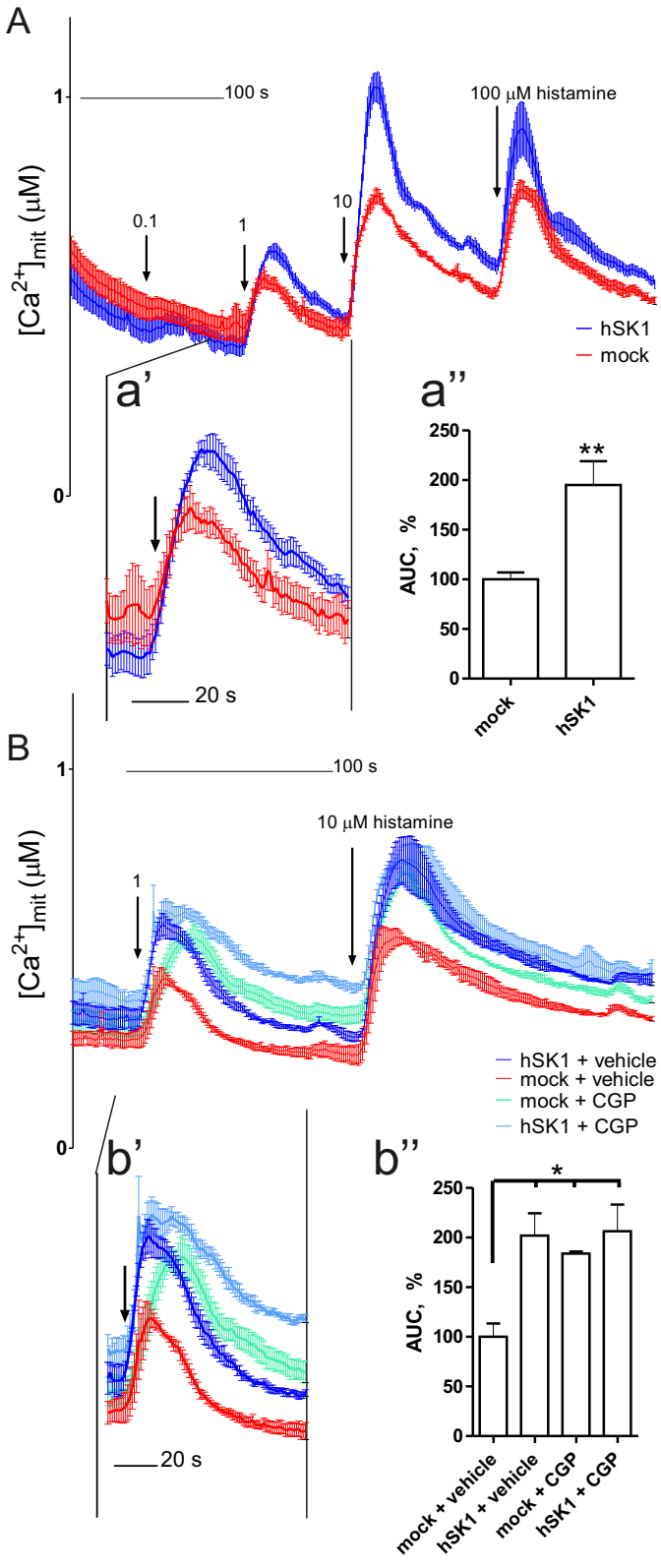

Fig. 4. SK1-overexpressing cell mitochondria accumulate Ca^{2+} more effectively than the mock-transduced control cells during stimulation with increasing histamine concentrations, and inhibition of the mitochondrial Na^+/Ca^{2+} exchanger NCLX augments mitochondrial Ca^{2+} retention in the mock-transduced cells. Mitochondria-targeted aequorin was employed in the Ca^{2+} experiments shown. A) SK1-overexpressing HeLa cells were treated with increasing histamine concentrations and mitochondrial matrix Ca^{2+} was measured. SK1 overexpression augmented $[Ca^{2+}]_{mit}$ during all stimulations. Area under curve (AUC) analysis was conducted on the selected timeframe of the experiment (a′) and quantified in (a″), N = 4. B) Inhibition of the mitochondrial Na^+/Ca^{2+} exchanger NCLX by CGP-37157 (CGP; 10 µM, 1 h) increases the accumulation of mitochondrial matrix Ca^{2+} in mock-transduced cells to a level resembling that of SK1-overexpressing cells. The AUC was analysed between the experimental time points shown in (b′) and the acquired values were analysed (b″), N = 4 vehicle-treated mock and hSK1, N = 3 for CGP-treated mock and hSK1. The average AUC from the shown time points is quantified in the bar diagrams and the error bars depict S.E.M. *P < 0.05, **P < 0.01.

cell proliferation [49]. However, SK1-overexpression did not affect proliferation (Fig. 7B). Finally, we observed an SK1-induced increase in cell migration (Fig. 7C). This finding is in line with the various mechanisms reported by which mitochondrial Ca^{2+} may regulate cell migration [50], and with the widely reported effects of SK1/S1P/S1P-receptor signaling on cancer cell migration and invasion [1,51,52].

3. Discussion

Aberrant sphingosine kinase 1/2 (SK1/2) expression and deregulated S1P signaling have been previously associated with severe conditions such as cancer, cardiovascular pathologies, inflammation, diabetes and neurological disorders [1,29]. Here, we show that SK1 overexpression modulates several important physiological parameters in HeLa cervical cancer cells. First, we show that SK1 overexpression significantly augments the IP_3-induced release of ER Ca^{2+}, and that the released Ca^{2+} is taken up by the mitochondria. The mechanisms underlying SK1-induced ER Ca^{2+} release and the following mitochondrial Ca^{2+} uptake could be many. Firstly, SK1 activation is modulated by Ca^{2+} [3]. Histamine-induced Ca^{2+} flux to the cytoplasm may thus activate SK1 leading to S1P production, which would amplify the IP_3 production in SK1-overexpressing cells through auto/paracrine stimulation of the G-protein coupled S1P-receptors. However, short-term blocking of the S1P receptors did not specifically abolish the effect of SK1 overexpression on mitochondrial Ca^{2+} (Suppl. Fig. 4A). Hence, the autocrine/paracrine S1P signaling loop does not play a major role here. S1P has been reported to have direct intracellular effects, including the release of Ca^{2+} from intracellular stores [3,53]. However, treatment with SK1 inhibitor (SKi, 10 µM, 1 h) did not abolish the effects of stable SK1 overexpression on mitochondrial Ca^{2+} (Suppl. Fig. 4B). Thus, instead of acute S1P-mediated effects, these findings indicated that SK1 overexpression has a long-term effect on ER-mitochondrial Ca^{2+} handling.

The robust increase in the $[Ca^{2+}]_{mit}$ induced by SK1 overexpression initially suggested that some of the recently characterized components of the mitochondrial calcium uniporter (MCU) might be affected [10,42]. However, no changes in the expression levels of the tested MCU components were found. In agreement with this, the intrinsic mitochondrial Ca^{2+} uptake capacity was not affected by SK1 overexpression. To further elucidate the nature of the SK1-mediated increase in $[Ca^{2+}]_{mit}$, we first treated the cells with ionomycin in the presence of the extracellular Ca^{2+} chelator EGTA (to induce rapid depletion of stored intracellular Ca^{2+}). In these conditions, SK1-overexpressing cells show higher $[Ca^{2+}]_{mit}$ than the mock-transduced cells. We then included a short incubation with the intracellular Ca^{2+} buffer BAPTA-AM in this experimental protocol [54]. The brief BAPTA-AM treatment blunted the ionomycin-induced mitochondrial Ca^{2+} uptake in mock-transduced cells, whereas the mitochondria in SK1-overexpressing cells were able to effectively accumulate Ca^{2+}. The results from the ionomycin treatments thus indicate an altered interaction between the mitochondria and the intracellular Ca^{2+} deposits (mainly the ER) in SK1-overexpressing cells. In addition, the previous finding that cytoplasmic Ca^{2+} was unaffected by SK1 overexpression upon ionomycin treatment (ref. [30]) corroborates the interpretation that SK1 somehow affects the Ca^{2+} flux between the ER and mitochondria.

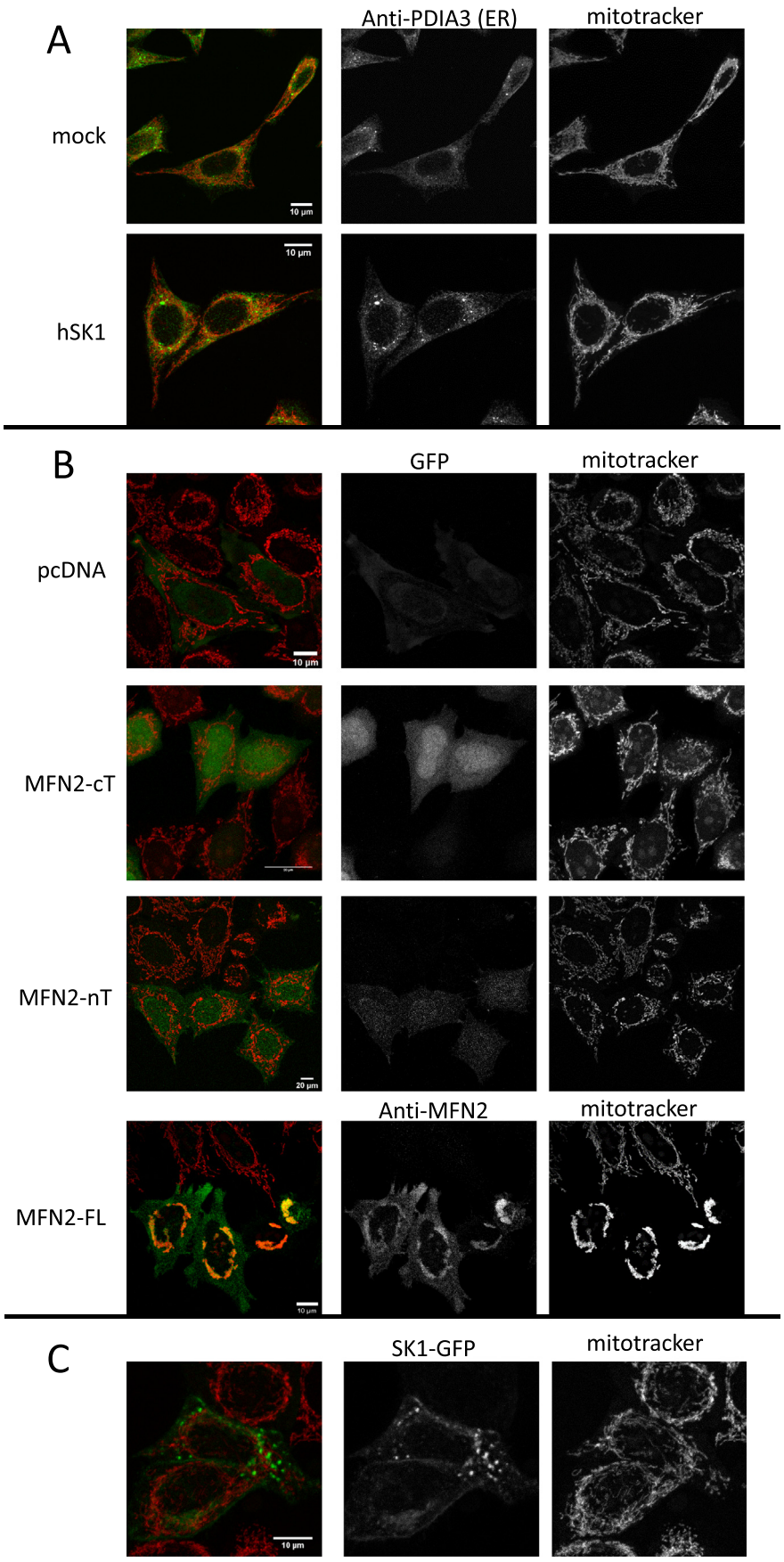

Fig. 5. Analysis of mitochondrial and ER network, as well as SK1 localization by employing confocal microscopy analysis. A) SK1-overexpression does not alter the mitochondria-ER network in HeLa cells. The panels show composite (left), anti-PDIA3 stained (ER-marker, middle) and mitotracker stained (right) representative confocal microscopy images. B) Control transfection (pcDNA) or MFN-2 C- or N-terminal (MFN2-cT; MFN2-nT) fragment overexpression do not alter the mitochondrial network, whereas full-length MFN-2 (MFN2-FL) overexpression leads to the previously reported clustering of mitochondria [44,48]. Co-expression of GFP with the pcDNA, MFN2-cT and MFN2-nT was employed to indicate the transfected cells. Mitochondrial network was visualized by mitotracker. Overexpressed MFN2 was detected by the anti-MFN2 antibody. C) SK1 does not localize to mitochondria in HeLa cells as evidenced by SK1-GFP and mitotracker.

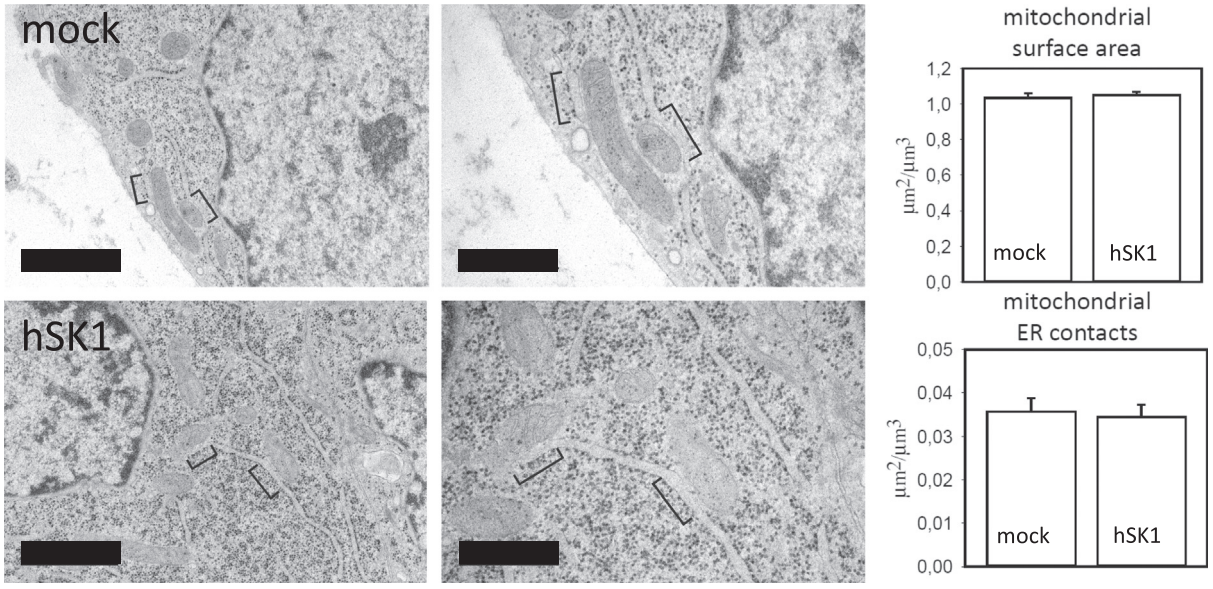

Fig. 6. Assessment of mitochondrial surface area and ER-mitochondrial contacts by electron microscopy. Areas of mitochondria-ER contact (brackets, at higher magnification at right) are equivalent in mock and hSK1 cells. The bar diagrams show the total surface area of mitochondria (µm2/µm3 of cytoplasm) and mitochondrial surface area in contact with the ER (µm2/µm3 of cytoplasm), respectively. Scale bar = 1 µm (left) and 500 nm (right). N = two independent experiment with 60 mock cell profiles and 60 hSK1 cell profiles analysed, respectively.

The results indicated that SK1 might modulate the ER-mitochondria interactions. However, confocal or electron microscopy revealed no changes in the ER-mitochondria organelle network or contacts, or mitochondrial surface area, upon SK1 overexpression. Nevertheless, we found that SK1 induces fragmentation of the MFN2 protein, which is a positive regulator of mitochondrial fusion, and, in addition, regulates the ER-mitochondria dynamics [14]. As mentioned before, whether MFN2 promotes or hinders the ER-mitochondria tethering is debated [14–20]. However, there is well-established evidence that MFN2 plays an important role in mitochondrial physiology [14]. Our results show that the expression of putative calpain-cleaved MFN2 N- and C- terminal fragments augments $[Ca^{2+}]_{mit}$ upon agonist stimulation. Intriguingly, a truncated, non-fusogenic form of MFN2 has been previously shown to have an effect on mitochondrial metabolism, and MFN2 fragments lacking the transmembrane domain re-establish mitochondrial targeting and activity when co-expressed with the C-terminal and the transmembrane domain MFN2 fragments [43,44]. Thus, MFN2 fragments are able to interact and retain (some degree) of their functionality. Also, short peptide fragments of MFN2 coiled-coil heptad repeat region (HR)-domains have been shown to bind to and modulate MFN2 functions [45]. Thus, protein fragments and/or peptide derivatives of MFN2 have been shown by others, and by us in the present study, to be biologically active. Further, glutamate-induced calpain activation has been shown to induce MFN2 degradation [39]. These findings are in line with our results showing an SK1-induced calpain activation and MFN2 fragmentation. Interestingly, calpain may localize to caveolae and we have previously shown that SK1-overexpression augments Ca^{2+} signaling at the caveolar sub-compartment without affecting the overall cytoplasmic Ca^{2+} [30,55]. As mentioned above, it is debated whether MFN2 antagonizes or augments mitochondrial Ca^{2+} [14–16]. Our results suggest that MFN2 fragment expression increases mitochondrial Ca^{2+}, but whether this effect is through inhibitory or

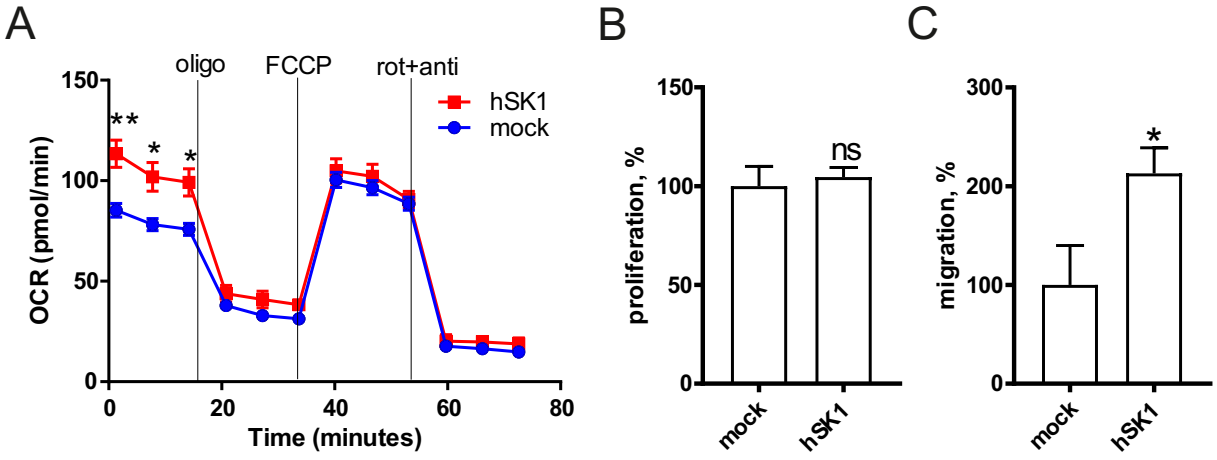

Fig. 7. Assessment of cell respiration, proliferation and migration. A) The basal oxygen consumption rate (OCR) in HeLa cells is augmented by SK1 overexpression. Oligo = 1 µM oligomycin, FCCP = 1 µM Trifluoromethoxy carbonylcyanide phenylhydrazone, rot = 0.5 µM rotenone, anti = 0.5 µM antimycin A. N = 5–6. B) Proliferation, as reported by a thymidine incorporation assay, is not affected by SK1 overexpression. *N* = 3. C) SK1 overexpression increases cell migration as reported by a Transwell migration assay. The cells were allowed to migrate for 12 h. N = 3. The bar diagrams show the average values with S.E.M, *P < 0.05, **P < 0.01.

activating interactions with endogenous MFN2, or through other effects, remains to be clarified.

Charcot-Marie-Tooth (CMT) disease is a neuropathy with multiple known contributing factors leading to the disease phenotype [56]. MFN2 mutations are associated with CMT type 2A (CMT2A) [57]. Interestingly, as evidenced by a *Drosophila* model, mutant MFN2 expression causes a CMT2A-resembling phenotype through excessive mitochondrial fusion or fission, respectively, depending on the site of mutation [58]. Further, S1P lyase deficiency is found in CMT patients, leading to increased S1P plasma levels [59]. SK1 overexpression might resemble S1P lyase deficiency as S1P levels are expected to increase in both conditions [1]. Also, disturbed Ca^{2+} homeostasis and mitochondrial dysfunction has been observed in a CMT model [60]. Given the recent pre-clinical advances in targeting mutant MFN2 in CMT2A models [57], and the fact that S1P signaling can be pharmacologically targeted [61], it would be interesting to test whether MFN2 is affected in patients with S1P lyase dysfunction.

MFN2 has been shown to modulate mitochondrial Ca^{2+} through affecting the activity of the mitochondrial matrix Ca^{2+}/Na^{+} exchanger NCLX in conditions where mitochondrial membrane potential is reduced [47]. Intriguingly, we found that mitochondrial membrane potential was reduced in SK1-overexpressing cells (Suppl. Fig. 3D). We observed that inhibition of NCLX did not significantly affect the mitochondrial Ca^{2+} dynamics in SK1-overexpressing cells, whereas the mock-transduced control cells showed increased accumulation of mitochondrial Ca^{2+} when extrusion of Ca^{2+} through NCLX was blocked. Also, it has been very recently reported that reduced mitochondrial membrane potential inhibits NCLX activity leading to accumulation of $[Ca^{2+}]_{mit}$ ([62]; NCLX regulation reviewed in [63]). It is therefore possible that altered NCLX activity in SK1-overexpressing cells might, in part, account for the observed increase in $[Ca^{2+}]_{mit}$.

The SK1-induced alterations in ER-mitochondrial Ca^{2+} handling may be of relevance in regard to the oncogenic functions of SK1, since the importance of Ca^{2+} signaling at the MAM sites in cancer is well-acknowledged [11,64]. The SK1-induced increase in mitochondrial matrix Ca^{2+} may affect cell energetics as $[Ca^{2+}]_{mit}$ regulates ATP production [10,65]. Further, mitochondrial Ca^{2+} has been shown to modulate cell migration [50]. Interestingly, we observed an SK1-mediated increase in cell respiration and migration, which is in agreement with the effects of altered $[Ca^{2+}]_{mit}$. The involvement of MFN2 in the regulation of mitochondrial Ca^{2+} is mechanistically complex and partially unclear as evidenced by multiple previous studies ([47], reviewed in [14]). Our data suggests that SK1, through fragmentation of MFN2 and possibly through the modulation of NCLX activity causes alterations in the mitochondrial Ca^{2+} handling. Further studies are needed to clarify the mechanistic details of MFN2 and mitochondrial Ca^{2+} dynamics. Taken together, our results show augmented mitochondrial Ca^{2+} uptake upon SK1 overexpression, with implications for the regulation of cell respiration and migration, providing novel insights to the oncogenic role of SK1 (schematic representation; Fig. 8).

4. Materials and methods

4.1. Cell culture, plasmids and transfections

HeLa [30] and human follicular thyroid cancer FTC-133 [66] cell lines were used in this study. The HeLa cells were grown in a humidified and thermostatic incubator with a controlled atmosphere (37 °C, 5% CO_2) in DMEM medium (#D6046, Sigma-Aldrich) supplemented with 10% fetal bovine serum and 1% penicillin/streptomycin (Life Sciences). The FTC-133 cells were cultured in DMEM and F12 (Ham's nutrient) medium (1:1) supplemented with 10% FBS, 1% P/S and 2 mM L-glutamine. Plasmid transfections were carried out by employing TurboFect (#R0531, Thermo Scientific) transfection reagent and OptiMEM media (#31985-070, Life Technologies), or by electroporation (4,000,000 cells with 20 μg of the desired plasmid suspended in 400 μL OptiMEM; 240 V; 500 μF). The stable SK1-overexpressing and mock-transduced HeLa cell lines, respectively, were created as described previously [30]. SK1-EGFP plasmid (SK1-GFP) was as described previously [67,68] the GFP plasmid (EGFP) was as in [69], and the GFP plasmid used in Fig. 5 was from Clontech (EGFP, #6085-1). Full length human MFN2, NT and CT fragments were cloned from human Nthy-ori 3.1 cell cDNA and inserted into pcDNA3 with *Hin*dIII and BamHI. All constructs were verified by Sanger sequencing. Primer sequences used are available upon request. Aequorin plasmids were as described in [31].

4.2. Ca^{2+} measurements

For compartment-specific Ca^{2+} measurements, we used luminescent aequorin chimeras [31] genetically targeted to the sarco/endoplasmic reticulum (mutated aequorin), to the mitochondrial matrix (wild-type aequorin) and to the cytoplasm (wild-type, no targeting sequence). These measurements were conducted as described previously by employing an in-house built luminometry setup or by utilizing a plate reader [31,69]. Briefly, the cells were plated either on to 12-well plates (100,000 cells per well) containing poly-L-lysine coated 13 mm coverslips, or, when employing a HIDEX Sense plate reader (HIDEX corp., Turku, Finland), on to 96-well plates (10,000 cells per well). The cells were transfected with the desired plasmid constructs (1 μg plasmid/ml medium, final total plasmid concentration on each well). Twenty-four hours post-transfection the cells were incubated in HBSS buffer (118 mM NaCl, 4.6 mM KCl, 10 mM glucose, 20 mM HEPES, pH 7.4) supplemented with 5 μM coelenterazine and 1 mM $CaCl_2$ (mitochondrial and cytoplasmic measurements) or 5 μM coelenterazine *n* along with 100 μM EGTA and 1 mM ionomycin (endo/sarcoplasmic measurements). Mitochondrial aequorin measurements in permeabilized cells were conducted exactly as described by Bonora et al. [31]. The cytoplasmic fluorescent Ca^{2+} indicator Fura-2-AM (Life Technologies) was employed as described in [69].

4.3. Western blot and antibodies

Western blotting was conducted as described previously [30]. Briefly, cells well were seeded onto 100 mm or 35 mm cell culture plates. At approximately 70% confluence, the cells were washed with phosphate buffered saline solution (PBS) and then harvested in a lysis buffer (10 mM Tris, 150 mM NaCl, 7 mM EDTA, 0.5% NP-40, 0.2 mM PMSF, and 0.5 μg/ml leupeptin, pH 7.7). The mitochondrial isolation was conducted as described in [70]. The lysates were supplemented with Laemmli sample buffer (LSB) and boiled for 5 min. The proteins were separated by SDS-PAGE and transferred to a nitrocellulose membrane by wet transfer. The membranes were incubated overnight with the primary antibodies and then with the horseradish peroxidase (HRP) –conjugated secondary antibodies. The protein bands were detected by chemiluminescence (WesternLightning, PerkinElmer, USA). The antibodies were: Anti-SK1 (Cell Signaling, #32975 [Suppl. Fig. 1] and #12071 [Suppl. Fig. 5]), Anti-Mitofusin-2 (M6319, Sigma-Aldrich), Anti-MCU antibody (HPA016480, MERCK), Pan-IP3R antibody IP3R1/2/3 H300 (sc-28613, Santa Cruz Biotechnology), Anti-CBARA1/MICU1 antibody (ab102830, Abcam), anti-GFP antibody (ab290, Abcam), AFG3L2 Polyclonal (#14631-1-AP, Proteintech), anti-OPA1, anti-MCUR1, Anti-mouse IgG HRP-linked secondary, Anti-Rat IgG HRP-linked secondary antibodies were from Cell Signaling Technology. Goat Anti-Rabbit IgG (H + L)-HRP Conjugate (#1706515, Biorad). Anti-HSC70 (ADI-SPA-815, Enzo Life Sciences) and anti-VDAC1 (MABN504, Merck) antibodies served as loading controls for whole cell and mitochondrial lysates, respectively. The anti-NCLX antibody [35] was a kind gift from professor Israel Sekler. The anti-IP3R1 (rbt03) antibody was described in [71]. In addition, antibodies that were used only for immunocytochemistry were: Anti-protein disulfide-isomerase A3

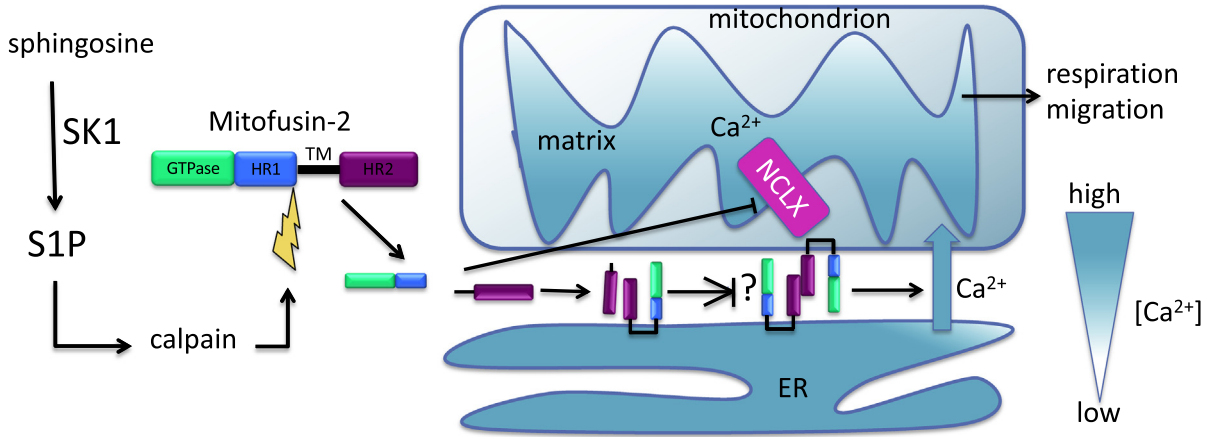

Fig. 8. Schematic representation of the proposed model. Sphingosine kinase 1 (SK1) phosphorylates sphingosine to form sphingosine 1-phosphate (S1P), which promotes calpain activation and consequent cleavage of mitofusin-2 (MFN2) at histidine 467. The cleaved fragments of MFN2 contain the functional GTPase and heptad-repeat 1 (HR1) domains, as well as the transmembrane (TM) and heptad-repeat 2 (HR2) domains, respectively. The MFN2 fragmentation modulates mitochondria-endoplasmic reticulum (ER) dynamics and inhibits the mitochondrial sodium-calcium (Ca^{2+}) exchanger NCLX, leading to increased mitochondrial matrix Ca^{2+} concentration ([Ca^{2+}]). Then, mitochondrial Ca^{2+} augments respiration and cell migration.

(PDIA3, AMAB90988, Sigma), Alexa Fluor 488 conjugate (A-11017 Mouse, A-11008 Rabbit, Life Technologies).

4.4. Cell migration and proliferation

Corning Transwell membrane inserts were employed to study cell migration according to a protocol modified from [72]. Briefly, 75,000 cells were collected in serum-free medium and allowed to migrate through uncoated Transwell membrane inserts for 12 h. Fetal bovine serum (FBS) was utilized as a chemoattractant. Then, the membranes were processed as described in [72] and the migrated cells were manually counted. The normalized cell counts were statistically analysed. Cell proliferation was measured by a thymidine incorporation assay at 48 h after seeding the cells as previously described in ref. [69].

4.5. Electron microscopy

For electron microscopy cells were fixed with 2.5% glutaraladehyde in 0.1 M cacodylate buffer, scraped and pelleted in gelatin, postfixed with 1% osmium tetroxide and 1.5% potassium ferrocyanide, dehydrated and embedded in an Epon resin. Ultrathin sections were poststained with uranyl acetate and lead citrate and 30 cell profiles from each culture were systematically sampled and photographed at 6000× with a Jeol JEM-1400 electron microscope equipped with a Gatan Orius SC 1000B bottom mounted CCD-camera. The pictures were viewed at a final magnification of 160,000×. A regular line grid was overlaid and the surface to volume ratios of mitochondrial outer surface membrane and mitochondrial membrane in close contact with the ER were determined according to the formula $S/V = 4c/lh$, where c is the number of times the lines intersected the surface of interest, h is the number of times the end points of the lines fell on cytoplasm and l is the length of a test line [73]. The graphs represent the results from 2 experiments ($n = 2$, in all 60 mock cell profiles, 60 hSK1 cell profiles).

4.6. Calpain activity assay

A calpain activity assay kit (#ab65308, Abcam, Cambridge, MA, USA) was employed. The assay was performed according to the manufacturer's instructions as described previously [66]. Briefly, 2,000,000 cells were grown overnight on 100-mm cell culture plates. The next day, the cells were detached and washed three times with PBS. Fluorescence was measured using a Hidex sense microplate reader instrument (HIDEX Corp, Turku, Finland) with the excitation light set at 400 nm and emitted light collected at 505 nm.

4.7. Cellular oxygen consumption measurements

For the oxygen consumption measurements, 10,000 HeLa cells per well were seeded onto a 96-well Agilent Seahorse XF Cell Mito Stress Test Kit plate and the measurements were conducted as defined in the manufacturer's protocol. To study the different mitochondrial respiration pathways, the cells were sequentially challenged with 1 μM oligomycin, 1 μM Trifluoromethoxy carbonylcyanide phenylhydrazone (FCCP) and 0.5 μM rotenone + 0.5 μM antimycin A, respectively.

4.8. Immunocytochemistry

The cells were seeded on 35 mm coverslips in 6-well plates the day before transfection. Cells were cultured and transfected as described in Section 4.1. Sixteen hours after transfection, the cells were incubated with MitoTracker-Red (MitoTracker® Red FM, M22425, Thermo) for 20 min, then fixed with 4% paraformaldehyde for 10 min at room temperature and rinsed in PBS three times. Permeabilization and block was performed in PBS containing 5% FBS and 0.3% (v/v) Triton X-100 for 5 min at room temperature. The cells were then incubated with appropriate primary antibodies (as listed below) for 90 min at 37 °C in the dark. After rinsing, the cells were incubated with corresponding secondary antibody for 1 h at 37 °C in the dark. All antibodies were diluted in blocking solution (5% FBS). The cells were then washed three times with PBS for 15 min and mounted with Vectashield Mounting Media with DAPI (H-1200, Vector Laboratories). Cells were imaged with 3i (Intelligent Imaging Innovations) CSU-W1 Confocal Spinning Disk Microscope (Yokogawa Corporation of America) equipped with Hamamatsu sCMOS Orca Flash 4 (Hamamatsu Photonics), using 63× oil immersion. Also used was Zeiss LSM 780 Confocal Microscope (Zeiss, Germany) with a 63× water immersion objective. The excitation/emission wavelengths (nm) used were: green (GFP), 498/516; and red (DsRed), 558/583. Image acquisition was performed with SlideBook v 6.0 and Zeiss Zen, respectively. Image processing was done using Fiji (ImageJ plugin collection) [74].

4.9. Mitochondrial membrane potential measurements

The cells were plated on to 24-well plates and treated on the next day with tetramethylrhodamine ethyl ester perchlorate (TMRE) for 20 min in the cell culture conditions as described in 4.1. The control

cells were treated with 100 μM FCCP 10 min prior to TMRE treatment. Thereafter, the cells were briefly washed in PBS containing 0.2% bovine serum albumin, and the TMRE fluorescence was read by utilizing a plate reader (HIDEX Sense, Hidex, Finland). Values obtained from a colorimetric crystal violet assay [75] was used to normalize the acquired TMRE fluorescence values.

4.10. Statistics

Statistical analysis was conducted by unpaired Student's *t*-test when two means were compared or by One-Way Anova with Tukey's post-hoc test when three or more means were compared. The GraphPad Prism 6 program (GraphPad Software Inc., San Diego, CA) was employed for the statistical analyses. A *P*-value below 0.05 was considered statistically significant.

Supplementary data to this article can be found online at https://doi.org/10.1016/j.bbamcr.2019.06.006.

Transparency document

The Transparency document associated with this article can be found, in online version.

Acknowledgements

I.P. received funding from the following foundations: Svenska Kulturfonden, the Magnus Ehrnrooths stiftelse, Finsk-Norska medicinska stiftelsen, Tor, Joe och Pentti Borgs Minnesfond, Oscar Öflunds stiftelse, Waldemar Von Frenckells stiftelse, K. Albin Johanssons stiftelse and Ida Montins stiftelse. J.H.N. was supported by Svenska Kulturfonden and the Otto A. Malm Foundation. D.M.T. received funding from the Sigrid Juséliuksen Säätiö and from the Novo Nordisk Foundation. K.T. was supported by the Sigrid Juséliuksen Säätiö and the Liv och Hälsa Foundation.

References

[1] B. Ogretmen, Sphingolipid metabolism in cancer signalling and therapy, Nat. Rev. Cancer 18 (2017) 33–50, https://doi.org/10.1038/nrc.2017.96.
[2] R. Brunkhorst, R. Vutukuri, W. Pfeilschifter, Fingolimod for the treatment of neurological diseases - state of play and future perspectives, Front. Cell. Neurosci. 8 (2014) 283, , https://doi.org/10.3389/fncel.2014.00283.
[3] I. Pulli, M.Y. Asghar, K. Kemppainen, K. Törnquist, Sphingolipid-mediated calcium signaling and its pathological effects, Biochim. Biophys. Acta, Mol. Cell Res. (2018), https://doi.org/10.1016/j.bbamcr.2018.04.012.
[4] K.E. Jarman, P.A.B. Moretti, J.R. Zebol, S.M. Pitson, Translocation of sphingosine kinase 1 to the plasma membrane is mediated by calcium- and integrin-binding protein 1, J. Biol. Chem. 285 (2010) 483–492, https://doi.org/10.1074/jbc.M109.068395.
[5] M. Brini, T. Calì, D. Ottolini, E. Carafoli, Neuronal calcium signaling: function and dysfunction, Cell. Mol. Life Sci. 71 (2014) 2787–2814, https://doi.org/10.1007/s00018-013-1550-7.
[6] M.J. Berridge, P. Lipp, M.D. Bootman, The versatility and universality of calcium signalling, Nat. Rev. Mol. Cell Biol. 1 (2000) 11–21, https://doi.org/10.1038/35036035.
[7] E.J. Griffiths, G.A. Rutter, Mitochondrial calcium as a key regulator of mitochondrial ATP production in mammalian cells, Biochim. Biophys. Acta Bioenerg. 1787 (2009) 1324–1333, https://doi.org/10.1016/J.BBABIO.2009.01.019.
[8] S. Marchi, S. Patergnani, S. Missiroli, G. Morciano, A. Rimessi, M.R. Wieckowski, C. Giorgi, P. Pinton, Mitochondrial and endoplasmic reticulum calcium homeostasis and cell death, Cell Calcium (2017), https://doi.org/10.1016/J.CECA.2017.05.003.
[9] D.E. Clapham, Calcium signaling, Cell. 131 (2007) 1047–1058, https://doi.org/10.1016/j.cell.2007.11.028.
[10] N. Nemani, S. Shanmughapriya, M. Madesh, Molecular regulation of MCU: implications in physiology and disease, Cell Calcium 74 (2018) 86–93, https://doi.org/10.1016/J.CECA.2018.06.006.
[11] M. Kerkhofs, M. Bittremieux, G. Morciano, C. Giorgi, P. Pinton, J.B. Parys, G. Bultynck, Emerging molecular mechanisms in chemotherapy: Ca2+ signaling at the mitochondria-associated endoplasmic reticulum membranes, Cell Death Dis. 9 (2018) 334, , https://doi.org/10.1038/s41419-017-0179-0.
[12] T. Balla, Ca 2+ and lipid signals hold hands at endoplasmic reticulum-plasma membrane contact sites, J. Physiol. (2018), https://doi.org/10.1113/JP274957.
[13] S. Muallem, W.Y. Chung, A. Jha, M. Ahuja, Lipids at membrane contact sites: cell signaling and ion transport, EMBO Rep. 18 (2017) e201744331, , https://doi.org/10.15252/embr.201744331.
[14] R. Filadi, E. Greotti, P. Pizzo, Highlighting the endoplasmic reticulum-mitochondria connection: focus on Mitofusin 2, Pharmacol. Res. 128 (2018) 42–51, https://doi.org/10.1016/J.PHRS.2018.01.003.
[15] D. Naon, M. Zaninello, M. Giacomello, T. Varanita, F. Grespi, S. Lakshminaranayan, A. Serafini, M. Semenzato, S. Herkenne, M.I. Hernández-Alvarez, A. Zorzano, D. De Stefani, G.W. Dorn, L. Scorrano, Critical reappraisal confirms that Mitofusin 2 is an endoplasmic reticulum–mitochondria tether, Proc. Natl. Acad. Sci. 113 (2016) 11249–11254, https://doi.org/10.1073/pnas.1606786113.
[16] R. Filadi, E. Greotti, G. Turacchio, A. Luini, T. Pozzan, P. Pizzo, Mitofusin 2 ablation increases endoplasmic reticulum–mitochondria coupling, Proc. Natl. Acad. Sci. 112 (2015) E2174–E2181, https://doi.org/10.1073/pnas.1504880112.
[17] P. Cosson, A. Marchetti, M. Ravazzola, L. Orci, Mitofusin-2 independent juxtaposition of endoplasmic reticulum and mitochondria: an ultrastructural study, PLoS One 7 (2012) e46293, , https://doi.org/10.1371/journal.pone.0046293.
[18] N.S. Leal, B. Schreiner, C.M. Pinho, R. Filadi, B. Wiehager, H. Karlström, P. Pizzo, M. Ankarcrona, Mitofusin-2 knockdown increases ER-mitochondria contact and decreases amyloid β-peptide production, J. Cell. Mol. Med. 20 (2016) 1686–1695, https://doi.org/10.1111/jcmm.12863.
[19] P.T.C. Wang, P.O. Garcin, M. Fu, M. Masoudi, P. St-Pierre, N. Panté, I.R. Nabi, Distinct mechanisms controlling rough and smooth endoplasmic reticulum contacts with mitochondria, J. Cell Sci. 128 (2015) 2759–2765, https://doi.org/10.1242/jcs.171132.
[20] Y. Chen, G. Csordas, C. Jowdy, T.G. Schneider, N. Csordas, W. Wang, Y. Liu, M. Kohlhaas, M. Meiser, S. Bergem, J.M. Nerbonne, G.W. Dorn, C. Maack, Mitofusin 2-containing mitochondrial-reticular microdomains direct rapid cardiomyocyte bioenergetic responses via Interorganelle Ca2+ crosstalk, Circ. Res. 111 (2012) 863–875, https://doi.org/10.1161/CIRCRESAHA.112.266585.
[21] G. Csordás, D. Weaver, G. Hajnóczky, Endoplasmic reticular–mitochondrial contactology: structure and signaling functions, Trends Cell Biol. (2018), https://doi.org/10.1016/J.TCB.2018.02.009.
[22] A. Vultur, C.S. Gibhardt, H. Stanisz, I. Bogeski, The role of the mitochondrial calcium uniporter (MCU) complex in cancer, Pflugers Arch. - Eur. J. Physiol. 470 (2018) 1149–1163, https://doi.org/10.1007/s00424-018-2162-8.
[23] L. Gomez, M. Paillard, M. Price, Q. Chen, G. Teixeira, S. Spiegel, E.J. Lesnefsky, A novel role for mitochondrial sphingosine-1-phosphate produced by sphingosine kinase-2 in PTP-mediated cell survival during cardioprotection, Basic Res. Cardiol. 106 (2011) 1341–1353, https://doi.org/10.1007/s00395-011-0223-7.
[24] G.M. Strub, M. Paillard, J. Liang, L. Gomez, J.C. Allegood, N.C. Hait, M. Maceyka, M.M. Price, Q. Chen, D.C. Simpson, T. Kordula, S. Milstien, E.J. Lesnefsky, S. Spiegel, Sphingosine-1-phosphate produced by sphingosine kinase 2 in mitochondria interacts with prohibitin 2 to regulate complex IV assembly and respiration, FASEB J. 25 (2011) 600–612, https://doi.org/10.1096/fj.10-167502.
[25] R. Fang, L. Zhang, L. Zhang, W. Li, M. Li, K. Wen, Sphingosine 1-phosphate postconditioning protects against myocardial ischemia/reperfusion injury in rats via mitochondrial signaling and Akt-Gsk3β phosphorylation, Arch. Med. Res. 48 (2017) 147–155, https://doi.org/10.1016/j.arcmed.2017.03.013.
[26] S. Kim, D. Sieburth, Sphingosine kinase activates the mitochondrial unfolded protein response and is targeted to mitochondria by stress, Cell Rep. 24 (2018) 2932–2945.e4, https://doi.org/10.1016/j.celrep.2018.08.037.
[27] S.-W. Hong, J. Lee, H. Kwon, S.E. Park, E.-J. Rhee, C.-Y. Park, K.-W. Oh, S.-W. Park, W.-Y. Lee, Deficiency of sphingosine-1-phosphate reduces the expression of prohibitin and causes β-cell impairment via mitochondrial dysregulation, Endocrinol. Metab. 33 (2018) 403, https://doi.org/10.3803/EnM.2018.33.3.403.
[28] J.-P. Decuypere, G. Monaco, G. Bultynck, L. Missiaen, H. De Smedt, J.B. Parys, The IP3 receptor–mitochondria connection in apoptosis and autophagy, Biochim. Biophys. Acta, Mol. Cell Res. 1813 (2011) 1003–1013, https://doi.org/10.1016/j.bbamcr.2010.11.023.
[29] S. Pyne, D.R. Adams, N.J. Pyne, Sphingosine 1-phosphate and sphingosine kinases in health and disease: recent advances, Prog. Lipid Res. 62 (2016) 93–106, https://doi.org/10.1016/J.PLIPRES.2016.03.001.
[30] I. Pulli, T. Blom, C. Lof, M. Magnusson, A. Rimessi, P. Pinton, K. Tornquist, A novel chimeric aequorin fused with caveolin-1 reveals a sphingosine kinase 1-regulated Ca(2)(+) microdomain in the caveolar compartment, Biochim. Biophys. Acta 1853 (2015) 2173–2182 doi https://doi.org/10.1016/j.bbamcr.2015.04.005.
[31] M. Bonora, C. Giorgi, A. Bononi, S. Marchi, S. Patergnani, A. Rimessi, R. Rizzuto, P. Pinton, Subcellular calcium measurements in mammalian cells using jellyfish photoprotein aequorin-based probes, Nat. Protoc. 8 (2013) 2105–2118, https://doi.org/10.1038/nprot.2013.127; 10.1038/nprot.2013.127.
[32] D. De Stefani, A. Raffaello, E. Teardo, I. Szabò, R. Rizzuto, A forty-kilodalton protein of the inner membrane is the mitochondrial calcium uniporter, Nature. 476 (2011) 336–340, https://doi.org/10.1038/nature10230.
[33] F. Perocchi, V.M. Gohil, H.S. Girgis, X.R. Bao, J.E. McCombs, A.E. Palmer, V.K. Mootha, MICU1 encodes a mitochondrial EF hand protein required for Ca2+ uptake, Nature. 467 (2010) 291–296, https://doi.org/10.1038/nature09358.
[34] K. Mallilankaraman, C. Cárdenas, P.J. Doonan, H.C. Chandramoorthy, K.M. Irrinki, T. Golenár, G. Csordás, P. Madireddi, J. Yang, M. Müller, R. Miller, J.E. Kolesar, J. Molgó, B. Kaufman, G. Hajnóczky, J.K. Foskett, M. Madesh, MCUR1 is an essential component of mitochondrial Ca2+ uptake that regulates cellular metabolism, Nat. Cell Biol. 14 (2012) 1336–1343, https://doi.org/10.1038/ncb2622.
[35] R. Palty, W.F. Silverman, M. Hershfinkel, T. Caporale, S.L. Sensi, J. Parnis, C. Nolte, D. Fishman, V. Shoshan-Barmatz, S. Herrmann, D. Khananshvili, I. Sekler, NCLX is an essential component of mitochondrial Na+/Ca2+ exchange, Proc. Natl. Acad. Sci. 107 (2010) 436–441, https://doi.org/10.1073/pnas.0908099107.
[36] F. Maltecca, D. De Stefani, L. Cassina, F. Consolato, M. Wasilewski, L. Scorrano, R. Rizzuto, G. Casari, Respiratory dysfunction by AFG3L2 deficiency causes

decreased mitochondrial calcium uptake via organellar network fragmentation, Hum. Mol. Genet. 21 (2012) 3858–3870, https://doi.org/10.1093/hmg/dds214.
[37] L. Fülöp, G. Szanda, B. Enyedi, P. Várnai, A. Spät, The effect of OPA1 on mitochondrial Ca2+ signaling, PLoS One 6 (2011) e25199, , https://doi.org/10.1371/journal.pone.0025199.
[38] R. Filadi, Di. Pendin, P. Pizzo, Mitofusin 2: from functions to disease, Cell Death Dis. 9 (2018), https://doi.org/10.1038/s41419-017-0023-6.
[39] W. Wang, F. Zhang, L. Li, F. Tang, S.L. Siedlak, H. Fujioka, Y. Liu, B. Su, Y. Pi, X. Wang, MFN2 couples glutamate excitotoxicity and mitochondrial dysfunction in motor neurons, J. Biol. Chem. 290 (2015) 168–182, https://doi.org/10.1074/jbc.M114.617167.
[40] N. Hagen, M. Hans, D. Hartmann, D. Swandulla, G. van Echten-Deckert, Sphingosine-1-phosphate links glycosphingolipid metabolism to neurodegeneration via a calpain-mediated mechanism, Cell Death Differ. 18 (2011) 1356–1365, https://doi.org/10.1038/cdd.2011.7.
[41] H. Kang, H.-I. Kwak, R. Kaunas, K.J. Bayless, Fluid shear stress and sphingosine 1-phosphate activate calpain to promote membrane type 1 matrix metalloproteinase (MT1-MMP) membrane translocation and endothelial invasion into three-dimensional collagen matrices, J. Biol. Chem. 286 (2011) 42017–42026, https://doi.org/10.1074/jbc.M111.290841.
[42] D.A. duVerle, Y. Ono, H. Sorimachi, H. Mamitsuka, Calpain cleavage prediction using multiple kernel learning, PLoS One 6 (2011) e19035, , https://doi.org/10.1371/journal.pone.0019035.
[43] J. Segales, J.C. Paz, M.I. Hernandez-Alvarez, D. Sala, J.P. Munoz, E. Noguera, S. Pich, M. Palacin, J.A. Enriquez, A. Zorzano, A form of mitofusin 2 (Mfn2) lacking the transmembrane domains and the COOH-terminal end stimulates metabolism in muscle and liver cells, AJP Endocrinol. Metab. 305 (2013) E1208–E1221, https://doi.org/10.1152/ajpendo.00546.2012.
[44] M. Rojo, F. Legros, D. Chateau, A. Lombes, Membrane topology and mitochondrial targeting of mitofusins, ubiquitous mammalian homologs of the transmembrane GTPase Fzo, J. Cell Sci. 115 (2002) 1663–1674, https://doi.org/10.1093/nar/25.17.3389.
[45] A. Franco, R.N. Kitsis, J.A. Fleischer, E. Gavathiotis, O.S. Kornfeld, G. Gong, N. Biris, A. Benz, N. Qvit, S.K. Donnelly, Y. Chen, S. Mennerick, L. Hodgson, D. Mochly-Rosen, G.W. Dorn, Correcting mitochondrial fusion by manipulating mitofusin conformations, Nature. 540 (2016) 74–79, https://doi.org/10.1038/nature20156.
[46] R. Palty, I. Sekler, The mitochondrial Na+/Ca2+ exchanger, Cell Calcium 52 (2012) 9–15, https://doi.org/10.1016/j.ceca.2012.02.010.
[47] K. Samanta, G.R. Mirams, A.B. Parekh, Sequential forward and reverse transport of the Na+ Ca2+ exchanger generates Ca2+ oscillations within mitochondria, Nat. Commun. 9 (2018) 156, , https://doi.org/10.1038/s41467-017-02638-2.
[48] D. Bach, S. Pich, F.X. Soriano, N. Vega, B. Baumgartner, J. Oriola, J.R. Daugaard, J. Lloberas, M. Camps, J.R. Zierath, R. Rabasa-Lhoret, H. Wallberg-Henriksson, M. Laville, M. Palacín, H. Vidal, F. Rivera, M. Brand, A. Zorzano, Mitofusin-2 determines mitochondrial network architecture and mitochondrial metabolism, J. Biol. Chem. 278 (2003) 17190–17197, https://doi.org/10.1074/jbc.M212754200.
[49] G. Bustos, P. Cruz, A. Lovy, C. Cárdenas, Endoplasmic reticulum-mitochondria calcium communication and the regulation of mitochondrial metabolism in cancer: a novel potential target, Front. Oncol. 7 (2017) 199, , https://doi.org/10.3389/fonc.2017.00199.
[50] V. Paupe, J. Prudent, New insights into the role of mitochondrial calcium homeostasis in cell migration, Biochem. Biophys. Res. Commun. 500 (2018) 75–86, https://doi.org/10.1016/J.BBRC.2017.05.039.
[51] S.N. Patmanathan, W. Wang, L.F. Yap, D.R. Herr, I.C. Paterson, Mechanisms of sphingosine 1-phosphate receptor signalling in cancer, Cell. Signal. 34 (2017) 66–75, https://doi.org/10.1016/J.CELLSIG.2017.03.002.
[52] N. Bergelin, T. Blom, J. Heikkilä, C. Löf, C. Alam, S. Balthasar, J.P. Slotte, A. Hinkkanen, K. Törnquist, Sphingosine kinase as an oncogene: autocrine sphingosine 1-phoshate modulates ML-1 thyroid carcinoma cell migration by a mechanism dependent on protein kinase C-α and ERK1/2, Endocrinology. 150 (2009) 2055–2063, https://doi.org/10.1210/en.2008-0625.
[53] D. Meyer zu Heringdorf, K. Liliom, M. Schaefer, K. Danneberg, J.H. Jaggar, G. Tigyi, K.H. Jakobs, Photolysis of intracellular caged sphingosine-1-phosphate causes Ca2+ mobilization independently of G-protein-coupled receptors., FEBS Lett. 554 (2003) 443–9. http://www.ncbi.nlm.nih.gov/pubmed/14623109 (accessed January 31, 2018).
[54] Y. Luo, J.D. Bond, V.M. Ingram, Compromised mitochondrial function leads to increased cytosolic calcium and to activation of MAP kinases, Proc. Natl. Acad. Sci. U. S. A. 94 (1997) 9705–9710.
[55] S. Goudenege, S. Poussard, S. Dulong, P. Cottin, Biologically active milli-calpain associated with caveolae is involved in a spatially compartmentalised signalling involving protein kinase C alpha and myristoylated alanine-rich C-kinase substrate (MARCKS), Int. J. Biochem. Cell Biol. 37 (2005) 1900–1910, https://doi.org/10.1016/J.BIOCEL.2005.04.010.
[56] J.C. Hoyle, M.C. Isfort, J. Roggenbuck, W.D. Arnold, The genetics of Charcot-Marie-Tooth disease: current trends and future implications for diagnosis and management, Appl. Clin. Genet. 8 (2015) 235–243, https://doi.org/10.2147/TACG.S69969.
[57] A.G. Rocha, A. Franco, A.M. Krezel, J.M. Rumsey, J.M. Alberti, W.C. Knight, N. Biris, E. Zacharioudakis, J.W. Janetka, R.H. Baloh, R.N. Kitsis, D. Mochly-Rosen, R. R. Townsend, E. Gavathiotis, G.W. Dorn, MFN2 agonists reverse mitochondrial defects in preclinical models of Charcot-Marie-Tooth disease type 2A, Science (80-.). 360 (2018) 336–341. doi:https://doi.org/10.1126/science.aao1785.
[58] N. El Fissi, M. Rojo, A. Aouane, E. Karatas, G. Poliacikova, C. David, J. Royet, T. Rival, Mitofusin gain and loss of function drive pathogenesis in *Drosophila* models of CMT2A neuropathy, EMBO Rep. (2018) e45241, , https://doi.org/10.15252/embr.201745241.
[59] D. Atkinson, J. Nikodinovic Glumac, B. Asselbergh, B. Ermanoska, D. Blocquel, R. Steiner, A. Estrada-Cuzcano, K. Peeters, T. Ooms, E. De Vriendt, X.L. Yang, T. Hornemann, V. Milic Rasic, A. Jordanova, Sphingosine 1-phosphate lyase deficiency causes Charcot-Marie-tooth neuropathy, Neurology. 88 (2017) 533–542, https://doi.org/10.1212/WNL.0000000000003595.
[60] M. Barneo-Muñoz, P. Juárez, A. Civera-Tregón, L. Yndriago, D. Pla-Martin, J. Zenker, C. Cuevas-Martín, A. Estela, M. Sánchez-Aragó, J. Forteza-Vila, J.M. Cuezva, R. Chrast, F. Palau, Lack of GDAP1 induces neuronal calcium and mitochondrial defects in a knockout mouse model of Charcot-Marie-Tooth neuropathy, PLoS Genet. 11 (2015) e1005115, , https://doi.org/10.1371/journal.pgen.1005115.
[61] A. Di Pardo, V. Maglione, Sphingolipid metabolism: a new therapeutic opportunity for brain degenerative disorders, Front. Neurosci. 12 (2018) 249, , https://doi.org/10.3389/fnins.2018.00249.
[62] M. Kostic, T. Katoshevski, I. Sekler, Allosteric regulation of NCLX by mitochondrial membrane potential links the metabolic state and Ca2+ signaling in mitochondria, Cell Rep. 25 (2018) 3465–3475.e4, https://doi.org/10.1016/J.CELREP.2018.11.084.
[63] M. Kostic, I. Sekler, Functional properties and mode of regulation of the mitochondrial Na+/Ca2+ exchanger, NCLX, Semin. Cell Dev. Biol. (2019), https://doi.org/10.1016/J.SEMCDB.2019.01.009.
[64] M. Kerkhofs, C. Giorgi, S. Marchi, B. Seitaj, J.B. Parys, P. Pinton, G. Bultynck, M. Bittremieux, Alterations in Ca2+ signalling via ER-mitochondria contact site remodelling in Cancer, Adv. Exp. Med. Biol. 997 (2017) 225–254, https://doi.org/10.1007/978-981-10-4567-7_17.
[65] L.S. Jouaville, P. Pinton, C. Bastianutto, G.A. Rutter, R. Rizzuto, Regulation of mitochondrial ATP synthesis by calcium: evidence for a long-term metabolic priming, Proc. Natl. Acad. Sci. U. S. A. 96 (1999) 13807–13812, https://doi.org/10.1073/PNAS.96.24.13807.
[66] M.Y. Asghar, K. Kemppainen, T. Lassila, K. Törnquist, Sphingosine 1-phosphate attenuates MMP2 and MMP9 in human anaplastic thyroid cancer C643 cells: importance of S1P2, PLoS One 13 (2018) e0196992, , https://doi.org/10.1371/journal.pone.0196992.
[67] S.M. Pitson, P.A.B. Moretti, J.R. Zebol, P. Xia, J.R. Gamble, M.A. Vadas, R.J. D'Andrea, B.W. Wattenberg, Expression of a catalytically inactive sphingosine kinase mutant blocks agonist-induced sphingosine kinase activation, J. Biol. Chem. 275 (2000) 33945–33950, https://doi.org/10.1074/jbc.M006176200.
[68] S.M. Pitson, R.J. D'andrea, L. Vandeleur, P.A. Moretti, P. Xia, J.R. Gamble, M.A. Vadas, B.W. Wattenberg, Human sphingosine kinase: purification, molecular cloning and characterization of the native and recombinant enzymes, Biochem. J. 350 (Pt 2) (2000) 429–441 http://www.ncbi.nlm.nih.gov/pubmed/10947957 , Accessed date: 4 March 2019.
[69] I. Pulli, T. Lassila, G. Pan, D. Yan, V.M. Olkkonen, K. Törnquist, Oxysterol-binding protein related-proteins (ORPs) 5 and 8 regulate calcium signaling at specific cell compartments, Cell Calcium 72 (2018) 62–69, https://doi.org/10.1016/j.ceca.2018.03.001.
[70] J.M. Gerhold, Ş. Cansiz-Arda, M. Lõhmus, O. Engberg, A. Reyes, H. van Rennes, A. Sanz, I.J. Holt, H.M. Cooper, J.N. Spelbrink, Human mitochondrial DNA-protein complexes attach to a cholesterol-rich membrane structure, Sci. Rep. 5 (2015) 15292, , https://doi.org/10.1038/srep15292.
[71] J.B. Parys, H. de Smedt, L. Missiaen, M.D. Bootman, I. Sienaert, R. Casteels, Rat basophilic leukemia cells as model system for inositol 1,4,5-trisphosphate receptor IV, a receptor of the type II family: functional comparison and immunological detection, Cell Calcium 17 (1995) 239–249 http://www.ncbi.nlm.nih.gov/pubmed/7664312 (accessed September 27, 2018).
[72] V. Kalhori, M. Magnusson, M.Y. Asghar, I. Pulli, K. Törnquist, FTY720 (Fingolimod) attenuates basal and sphingosine-1-phosphate-evoked thyroid cancer cell invasion, Endocr. Relat. Cancer 23 (2016), https://doi.org/10.1530/ERC-16-0050.
[73] E.R. Weibel, Stereological Methods, Academic Press, 1979, https://www.ncbi.nlm.nih.gov/nlmcatalog/8007268 (accessed March 28, 2018).
[74] J. Schindelin, I. Arganda-Carreras, E. Frise, V. Kaynig, M. Longair, T. Pietzsch, S. Preibisch, C. Rueden, S. Saalfeld, B. Schmid, J.-Y. Tinevez, D.J. White, V. Hartenstein, K. Eliceiri, P. Tomancak, A. Cardona, Fiji: an open-source platform for biological-image analysis, Nat. Methods 9 (2012) 676–682, https://doi.org/10.1038/nmeth.2019.
[75] M. Thomas, C.E. Finnegan, K.M. Rogers, J.W. Purcell, A. Trimble, P.G. Johnston, M.P. Boland, STAT1: A Modulator of Chemotherapy-Induced Apoptosis, (2004), pp. 8357–8364.